

# STUDY OF TRANSVERSE RESONANCE ISLAND BUCKETS AT CESR\*

S. T. Wang<sup>†</sup>, V. Khachatryan, CLASSE, Cornell University, Ithaca, NY, USA

## Abstract

A 6-GeV lattice with the horizontal tune near a 3rd-order resonance line at  $3\nu_x=2$  is designed for studying the transverse resonance island buckets (TRIBs) at the Cornell Electron Storage Ring (CESR). The distribution of 76 sextupoles powered individually is optimized to maximize the dynamic aperture and achieve the desired amplitude-dependent tune shift  $\alpha_{xx}$  and the resonant driving term  $h_{30000}$ , which are necessary conditions to form stable island buckets. The particle tracking simulations are developed to check and confirm the formation of TRIBs at different tunes with clearing kicks in this TRIBs lattice. Finally, the lattice is loaded in CESR and the TRIBs are successfully observed when the horizontal fractional tune is adjusted to 0.665, close to the 3rd-order resonance line. Bunch-by-bunch feedback is also explored to clear the particles in the main bucket and the island buckets, respectively.

## INTRODUCTION

Nonlinear resonances are critical topics in the beam dynamics of accelerator physics, which have been studied theoretically and experimentally for many years [1]. Normally a storage ring operates at tunes far away from resonant lines to avoid the negative impact such as instability, poor lifetime, and increased emittance. However, by taking advantage of the resonance nature, one application of the ring operating at the 3rd-order resonance line is to extract particles in multi-turns at CESR-PS and ELSA [2]. Recently, MLS and BESSY-II have demonstrated the stable two-orbit operation by utilizing the transverse resonance island buckets (TRIBs) [3, 4]. The second orbit for the beam in the island decreased the x-ray pulse frequency by 3 or 4 times which expands the possibilities for timing experiments [5].

TRIBs form in the vicinity of a resonance line, which can be achieved by adjusting the horizontal tune along with the families of sextupoles (harmonic and normal) to tune the amplitude-dependent tune shift (ADTS) to stabilize the beam [3]. This approach is effective but empirical tuning of the sextupoles may be required. With this method, TRIBs have been successfully observed at MLS, BESSY-II, and MAX-IV [6]. To understand how TRIBs can form at CESR, a relatively high-energy (6-GeV) storage ring, we choose a different approach by designing a lattice with the horizontal tune near the 3rd integer line and a new sextupole distribution, at which TRIBs could form easily by adjusting the horizontal tune only.

In this paper, we discuss the criteria of optimizing the sextupoles for the TRIBs. A particle tracking simulation is developed to demonstrate the formation of TRIBs at different

tunes. The lattice is then loaded into CESR and the TRIBs are successfully observed while adjusting horizontal tune to 0.665. Clearing kicks using feedback kicker is explored to clear the particles in the core or island buckets.

## LATTICE DESIGN

Cornell Electron Storage Ring (CESR) is a 6-GeV accelerator located on the Cornell University campus. Since 2008, CESR serves as a dedicated light source for x-ray users, namely Cornell High Energy Synchrotron Source (CHESS). In 2018, one sextant of the ring was upgraded with double bend acromat to reduce the emittance and accommodate more compact undulators [7]. The main accelerator parameters are listed in Table 1. CESR magnets including 113 quadrupoles, 12 dipole quadrupoles, and 76 sextupoles are all individually powered, which provides great flexibility for lattice design and complex nonlinear dynamics studies. Details of CESR lattice are described in Ref [7].

As shown in Table 1, the nominal horizontal fractional tune ( $Q_x$ ) during CHESS operation is 0.556, far from the 3rd-order line  $3\nu_x=2$  (0.667). It is very unlikely that TRIBs would appear by only adjusting the tune near 0.667. Thus, we first optimize quadrupoles to create a linear lattice with the design tunes at (16.643, 12.579) closer to the 3rd-order line while preserving most optics parameters as the normal lattice. Then 76 sextupoles are optimized to meet the conditions of forming TRIBs as well as maximizing the dynamic aperture (DA).

The formula of the stable fixed points (SFP) have been derived in Reference [1] as shown in Eq. (1),

$$J_{SFP}^{1/2} = \frac{3G_{3,0,l}}{4\alpha_{xx}} \left( 1 \pm \sqrt{1 - \frac{16\alpha_{xx}\delta}{9G_{3,0,l}^2}} \right), \quad (1)$$

where  $J_{SFP}$  is the particle's action at the SFP,  $G_{3,0,l}$  is the resonance strength at the 3rd-order resonance  $3\nu_x=l$ ,  $\alpha_{xx}$  is the detune coefficient of ADTS, and  $\delta=Q_x - \frac{l}{3}$ . As Eq. (1) implies, the formation of TRIBs depends on three variables

Table 1: CESR Parameters

Beam Energy (GeV)	$E_0$	6.0
Circumference (m)	$L$	768.438
Transverse Damping time (ms)	$\tau_{x,y}$	12.0, 14.6
Longitudinal Damping time (ms)	$\tau_z$	8.2
Synchrotron tune	$Q_s$	0.027
Horizontal tune	$Q_x$	16.556
Vertical Tune	$Q_y$	12.636
Horizontal Emittance (nm-rad)	$\epsilon_x$	$\sim 28$
Energy spread	$\sigma_p$	$8.2 \times 10^{-4}$

\* Work supported by NSF PHYS-1757811 and DMR-1829070.

<sup>†</sup> sw565@cornell.edu

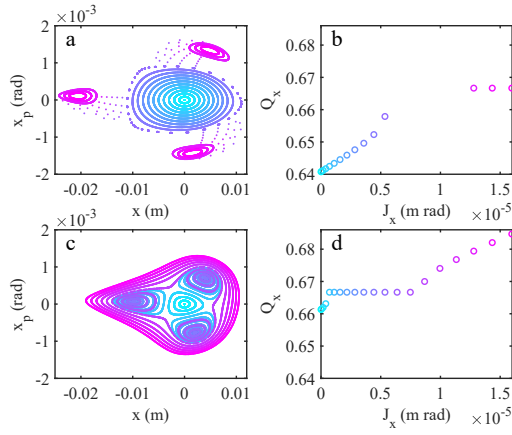


Figure 1: Particles'  $xx_p$  plots at two lattice tunes (a)  $Q_x=0.643$  and (c)  $0.661$ . The particle's  $Q_x$  as a function of its action in (b) and (d) are calculated from the TBT data plotted in (a) and (c), respectively.

$G_{3,0,l}$ ,  $\alpha_{xx}$ , and  $Q_x$ . Thus, adjusting the tune ( $Q_x$ ) and the ADTS ( $\alpha_{xx}$ ) will help the formation of TRIBs.

For sextupole optimization, appropriate target values of  $G_{3,0,l}$  and  $\alpha_{xx}$  are needed. Suppose we approach the 3rd-order line from below and observe TRIBs at  $Q_x=0.654$  ( $\delta=-0.013$ ) with  $J_{SFP}=1.0 \times 10^{-5}$  m-rad, which is within the range that our instrument [8] can measure the TRIBs. Since  $\delta < 0$ ,  $\alpha_{xx} > 0$  will satisfy the bifurcation condition  $\frac{16\alpha_{xx}\delta}{9G_{3,0,l}^2} \leq 1$  more easily. Using Eq. (1) with the above requirements, we obtain one set of values  $G_{3,0,l}=0.1$  and  $\alpha_{xx}=1347$  for the sextupole optimization. In the optimization requirement, resonant driving terms except  $h_{30000}$  and  $h_{22000}$ , which are directly related to  $G_{3,0,l}$  and  $\alpha_{xx}$ , respectively, are minimized to maximize the DA. The horizontal and vertical chromaticities are fixed at 1.

## SIMULATION

Once the linear lattice with desired sextupoles are optimized, simulations are implemented to check the lattice properties. All the simulation programs discussed below are based on BMAD code library [9]. First, 20 particles with different action are tracked through the TRIBs lattice at different  $Q_x$  for 1000 turns while RF, radiation damping and excitation are turned off. Figure 1 (a) and (c) plot the  $xx_p$  of all particles at  $Q_x=0.643$  and  $0.661$ , respectively. Three stable islands are clearly visible at both tunes in the phase space. From FFT analysis of the turn-by-turn (TBT)  $x$  coordinates, the particles'  $Q_x$  are calculated and shown as a function of their actions in Fig. 1 (b) and (d). Both plots show that  $Q_x$  increases as the particle's action increases, indicating a positive ADTS coefficient ( $\alpha_{xx} > 0$ ). When the particles are in the stable islands, their tunes are exactly  $2/3$ . Several particles are lost while tracking through the lattice with  $Q_x=0.643$  so that their tunes are absent in Fig. 1 (b).

From the  $xx_p$  phase space plots in Fig. 1, the action of SFP at different  $Q_x$  is extracted and plotted in Fig. 2. The

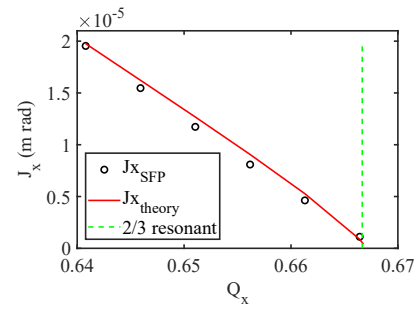


Figure 2: The particle action at the SFP as a function of lattice tune.

extracted  $J_{x,SFP}$  decreases as the tune approaches the 3rd-order resonance line, indicating the island separation in the horizontal plane shrinks. The simulated  $J_{x,SFP}$  agrees very well with the calculated  $J_{x,theory}$  using Eq. (1).

Frequency map analysis is performed to check the DA of the TRIBs lattice at different tunes. Figure 3 (a) and (b) show the DA at  $Q_x=0.643$  and  $0.661$ , respectively. It is interesting that both the island and main buckets are visible in these plots. The horizontal DA of the island bucket is much less than the main buckets at  $Q_x=0.643$  while comparable to the main bucket at  $Q_x=0.661$ , which is consistent with the phase space plots in Fig. 1.

More realistic tracking simulation including radiation damping and excitation is implemented to check the TRIBs formation in the TRIBs lattice. Starting with an initial distribution with design emittance  $\epsilon_x=30$  nm-rad (Fig. 4 (a)), 1000 particles are tracked through the lattice at different horizontal tunes. Since the horizontal radiation damping time in CESR

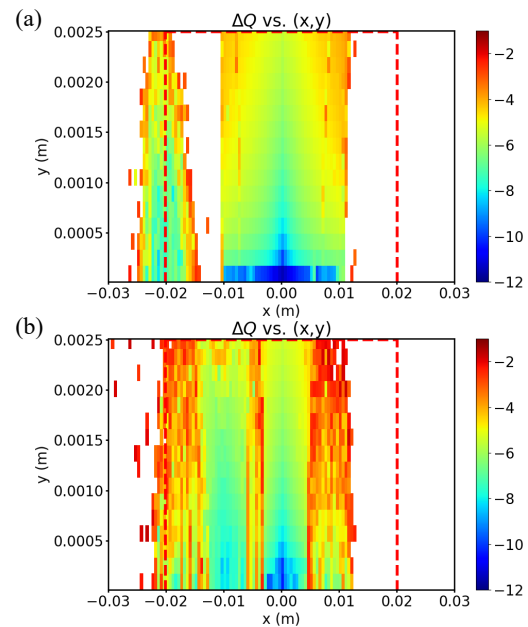


Figure 3: Dynamic aperture at two different horizontal tunes (a)  $Q_x=0.643$  and (b)  $0.661$ . The red dash lines indicate the physical apertures at element 1.

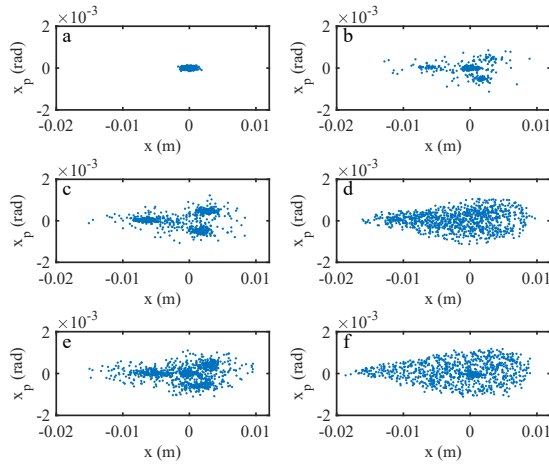


Figure 4: The 1000-particles distribution in the  $xx_p$  phase space at  $Q_x=0.6649$  (259.4 kHz) at (a) turn 1 and (b) turn 40000, when applying a sinusoidal kick at  $f=259.4$  kHz with the kick amplitude of (c)  $0.5 \mu\text{rad}$  and (d)  $5 \mu\text{rad}$  at turn 40000, and at  $f=261.35$  kHz with the kick amplitude of (e)  $0.5 \mu\text{rad}$  and (f)  $5 \mu\text{rad}$  at turn 40000.

is  $12 \text{ ms}$  ( $\sim 5000$  turns),  $4 \times 10^4$  turns is used for tracking to cover  $\sim 8$  damping times. When  $Q_x < 0.6613$  (258 kHz), the particles remain in the similar distribution through  $4 \times 10^4$  turns as seen in Fig. 4 (a). When  $Q_x > 0.6639$  (259 kHz), the particles diffuse from the core to the island buckets. Figure 4 (b) shows the particles occupy three islands as well as the core after tracking  $4 \times 10^4$  turns at  $Q_x=0.6649$  (259.4 kHz).

Starting with the distribution in Fig. 4 (b) and applying a sinusoidal kick at  $f=259.4$  kHz same as the core tune, most particles are driven from the core to island buckets (Fig. 4 (c)) after tracking  $4 \times 10^4$  turns. However when the sinusoidal kick amplitude is greater than  $3 \mu\text{rad}$ , the particles are not clustered in the islands but distributed in the  $xx_p$  space evenly (Fig. 4 (d)).

When starting tracking with the initial distribution as in Fig. 4 (c) with the sinusoidal kick at  $f=261.35$  kHz near the island tune (0.667), the particles are converged back to the core bucket but not fully cleared from the islands buckets after  $4 \times 10^4$  turns (Fig. 4 (e)). When increasing the kick amplitude to  $5 \mu\text{rad}$ , the particles are cleared from island buckets but most of them are evenly distributed in the phase space (Fig. 4 (f)).

## EXPERIMENT

After confirming the formation of TRIBs in simulation, we loaded the TRIBs lattice into CESR. Once the optics correction were made (phase and orbit), we adjusted  $Q_x$  from 0.6537 to 0.667 while viewing and recording the beam profile from synchrotron radiation using vBSM [8]. The beam profile images from a 1-mA single positron bunch observed at different tunes are shown in Fig. 5. When  $Q_x < 0.663$  (258.7 kHz), the beam stays in the core (Fig. 5 (a)). When

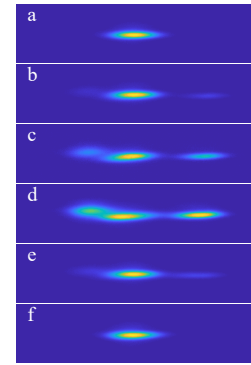


Figure 5: Beam profiles at  $Q_x=$  (a) 0.6613 (258.0 kHz), (b) 0.6631 (258.7 kHz), (c) 0.6648 (259.35 kHz), and (f) 0.6700 (261.4 kHz). (d) and (e) are recorded at the same tune 0.6638 (259.35 kHz) but with applying a sinusoidal kick at  $f=259.35$  kHz and 261.35 kHz, respectively.

$Q_x$  is near 0.663 (258.7 kHz), the TRIBs start to form (Fig. 5 (b)) while most particles are still in the core bucket. When  $Q_x=0.6648$  (259.35 kHz), more particles diffuse to the island buckets (Fig. 5 (c)). A bunch-by-bunch feedback was then used to apply a sinusoidal kick ( $\sim 0.1 \mu\text{rad}$ ) with the same frequency as the core tune 259.35 kHz to the beam. This clearing kick drives the particles from the core to the island buckets (Fig. 5 (d)). If the sinusoidal kick's frequency was set to 261.35 kHz, this clearing kick drives the particles from the islands to the core (Fig. 5 (e)). But there are still some particles remaining in the island buckets. When  $Q_x$  is above the 3rd-order resonant line 0.667 (260.1 kHz), all the particles diffuse back to the core island (Fig. 5 (f)). The experimental observation agrees well with the simulation results. The behavior of the clearing kick is consistent with the results reported in Ref [3].

## CONCLUSION

We studied the conditions of TRIBs formation near a 3rd-order resonance line and designed a special lattice with optimized sextupole distribution to meet the requirement. Tracking simulation is then developed to confirm the formation of TRIBs. Finally, the lattice was loaded into CESR and the TRIBs were observed at  $Q_x=0.6648$  (259.35 kHz). In addition, the sinusoidal kicks at 259.35 kHz or 261.3 kHz help to clear the particles in the core or island buckets, respectively. In conclusion, we have demonstrated a new approach to design and observe TRIBs in a high-energy storage ring, which provides guidance for future systematic TRIBs study.

## ACKNOWLEDGMENTS

We thank David Rubin and Robert Meller for valuable discussion, Joel Brock and Ernest Fontes for supporting the project.

## REFERENCES

- [1] S.Y. Lee, “Accelerator Physics,” World Scientific, 1999, p. 183–193. doi:10.1142/3977
- [2] R. Capii and M. Giovannozzi, “Multiturn extraction and injection by means of adiabatic capture in stable islands of phase space,” *Phys. Rev. ST Accel. Beams*, vol. 7, p. 024001, 2004.
- [3] M. Ries *et al.*, “Transverse Resonance Island Buckets at the MLS and BESSY II”, in *Proc. IPAC’15*, Richmond, VA, USA, May 2015, pp. 138–140. doi:10.18429/JACoW-IPAC2015-MOPWA021
- [4] P. Goslawski *et al.*, “Two Orbit Operation at Bessy II - During a User Test Week”, in *Proc. IPAC’19*, Melbourne, Australia, May 2019, pp. 3419–3422. doi:10.18429/JACoW-IPAC2019-THYYPLM2
- [5] K. Holldack *et al.*, “Flipping the helicity of X-rays from an undulator at unprecedented speed,” *Communications physics*, vol. 3, p. 61, 2020. <https://doi.org/10.1038/s42005-020-0331-5>
- [6] P. F. Tavares *et al.*, “Status of the MAX IV Accelerators”, in *Proc. IPAC’19*, Melbourne, Australia, May 2019, pp. 1185–1190. doi:10.18429/JACoW-IPAC2019-TUYPLM3
- [7] J. Shanks *et al.*, “Accelerator design for the Cornell High Energy Synchrotron Source upgrade,” *Phys. Rev. ST Accel. Beams*, vol. 22, p. 021602, 2019.
- [8] S. T. Wang *et al.*, “Visible-Light Beam Size Monitors Using Synchrotron Radiation at CESR,” *Nucl. Instrum. Methods Phys. Res., Sect. A*, vol. 703, pp. 80–90, Mar. 2013.
- [9] D. Sagan, “Bmad: A relativistic charged particle simulation library,” *Nucl. Instrum. Methods Phys. Res., Sect. A*, vol. 558, p. 356, 2006.